Are fast radio bursts the most likely electromagnetic counterpart of neutron star mergers resulting in prompt collapse?

Vasileios Paschalidis[1] and Milton Ruiz[2]

[1]*Departments of Astronomy and Physics, University of Arizona, Tucson, Arizona 85719, USA*
[2]*Department of Physics, University of Illinois at Urbana-Champaign, Urbana, Illinois 61801, USA*

(Received 11 August 2018; published 1 August 2019)

Inspiraling and merging binary neutron stars (BNSs) are important sources of both gravitational waves and coincident electromagnetic counterparts. If the BNS total mass is larger than a threshold value, a black hole ensues promptly after merger. Through a statistical study in conjunction with recent LIGO/Virgo constraints on the nuclear equation of state, we estimate that up to ∼25% of BNS mergers may result in prompt collapse. Moreover, we find that most models of the BNS mass function we study here predict that the majority of prompt-collapse BNS mergers have $q \gtrsim 0.8$. Prompt-collapse BNS mergers with mass ratio $q \gtrsim 0.8$ may not be accompanied by detectable kilonovae or short gamma-ray bursts, because they unbind a negligible amount of mass and form negligibly small accretion disks onto the remnant black hole. We call such BNS mergers "orphan." However, recent studies have found that $10^{41-43}(B_p/10^{12}\ \mathrm{G})^2\ \mathrm{erg\,s^{-1}}$ electromagnetic signals can be powered by magnetospheric interactions several milliseconds prior to merger. Moreover, the energy stored in the magnetosphere of an orphan BNS merger remnant will be radiated away in $\mathcal{O}(1\ \mathrm{ms})$. Through simulations in full general relativity of BNSs endowed with an initial dipole magnetosphere, we find that the energy in the magnetosphere following black hole formation is $E_B \sim 10^{39-41}(B_p/10^{12}\ \mathrm{G})^2$ erg. Radiating ∼1% of E_B in 1 ms, as has been found in previous studies, matches the premerger magnetospheric luminosity. These magnetospheric signals are not beamed, and their duration and power agrees with those of nonrepeating fast radio bursts (FRBs). These results combined with our statistical study suggest that a nonrepeating FRB *may* be the most likely electromagnetic counterpart of prompt-collapse BNSs. Detection of a nonrepeating FRB coincident with gravitational waves from a BNS merger could settle the extragalactic origin of a fraction FRBs and could be used to place constraints on the nuclear equation of state. FRBs can also initiate triggered searches for weak signals in the LIGO/Virgo data.

DOI: 10.1103/PhysRevD.100.043001

I. INTRODUCTION

The LIGO and Virgo collaborations have already reported the direct detection of gravitational waves (GWs) from the inspiral and merger of a number of binary black holes [1–6] and one binary neutron star (BNS) [7] (event GW170817), that was accompanied by multiple electromagnetic (EM) counterparts [8,9]. The consequences for astrophysics and fundamental physics from these observations are far reaching, and it is a matter of time until the detection of such compact binaries becomes routine.

Merging BNSs are not only important sources of GWs, but also sources of coincident EM counterparts. These systems had long been suspected as the progenitors of short gamma-ray bursts (sGRBs) [10–21]. The detection of the GW170817-counterpart GRB170817A [8] has provided the best evidence, yet, that some sGRBs are powered by BNSs. BNSs are also sources of kilonovae/macronovae [22,23]. The association of kilonova AT 2017gfo/DLT17ck with GW170817 [9] has verified this expectation, too.

Merging BNSs may also be progenitors for *fast radio bursts* (FRBs)—a new class of radio transients lasting between a few to a couple of tens of milliseconds [24,25]. So far 78 FRBs have been detected [26]. The existence of two repeating FRBs "FRB121102" [27] (which has also been detected recently by CHIME [28]) and "FRB 180814.J0422 + 7" [29] points to a noncatastrophic origin as opposed to a collapse or merger, which suggests that there may be at least two different classes of FRB progenitors. Several models have been proposed to explain FRBs including magnetar giant flares, coherent radiation from magnetic braking at BNS merger, blitzars (collapsing supramassive NSs), dark-matter induced collapse of NSs, axion-miniclusters, newborn highly magnetized NSs in supernova remnants, black hole–neutron star batteries, charged black hole (BH) binaries, black hole current sheets, black hole superradiance induced by plasma [30–44].

Kilonovae from BNS mergers require dynamical ejection of matter during merger and/or from an accretion disk by neutrino irradiation, see e.g., [45] for a review. It is also

widely accepted that BNSs can generate sGRBs, if a jet is launched by the BH-disk engine that forms following merger. Thus, in a scenario where a negligibly small disk forms, and a negligible amount of mass escapes, one may expect no sGRB and/or an undetectable kilonova from the BNS event. We will refer to such "kilonova-free" and "sGRB-free" BNS mergers that are detected in the GW spectrum as "orphan." However, we stress the term orphan will be used to only mean that any potential accompanying kilonova/sGRB is sub-threshold, and not that they do no exist. Note also that there exist "orphan afterglows" of sGRBs, where the gamma-rays are not detected (they are subthreshold), but the radio afterglow is detected (see, e.g., [46]). But, are there any scenarios where such orphan BNS mergers arise?

Numerical relativity simulations have shown that when the BNS total mass ($M_{\rm tot}$) is greater than a threshold mass ($M_{\rm thres}$), a BH ensues in the first millisecond after merger. In this prompt-collapse scenario a negligible amount of matter is ejected dynamically [47] (see also [48]) and a negligible amount of matter is available to form a disk [47,49–52]. Negligibly small disks were also reported in [53], where it was demonstrated that in prompt-collapse BNS mergers a jet cannot be launched as opposed to the "delayed" collapse scenario which forms massive disks [19,54]. For illustration we note that ejecta masses ~ 0.025–$0.05 M_\odot$ are required to explain the kilonova associated with GW170817 [55–65], while typical ejecta from equal-mass, prompt-collapse BNS mergers are $\mathcal{O}(10^{-4} M_\odot)$ or less [47,66] [67], and disk masses $\mathcal{O}(10^{-3} M_\odot)$ [52]. According to [68] ejecta masses $\mathcal{O}(10^{-3} M_\odot)$ or greater are required for detectable kilonovae at the depth and cadence of the normal LSST survey with current or planned telescopes. Therefore, prompt-collapse BNS mergers may appear orphan unless they take place nearby. This raises the main question that we focus on in this paper: what is the most likely electromagnetic counterpart of orphan prompt-collapse BNS mergers?

First, we point out that if the binary mass ratio q (defined here to be less than unity) is smaller than 0.8, then both appreciable matter may become unbound and a sizable disk onto the remnant BH may form [47,48,69]. This is because for substantially asymmetric BNSs the lighter companion is tidally disrupted before merger, in contrast to near equal-mass binaries. Thus, sufficiently asymmetric, prompt-collapse BNS mergers may power both sGRBs and kilonovae.

In this work we perform a statistical study to assess the astrophysical relevance of prompt-collapse BNSs, and the likelihood of orphan BNS mergers. In particular, we compute the $M_{\rm tot}$ and q distribution of BNSs using the Galactic NS mass function and population synthesis models in conjunction with GW170817 constraints on the nuclear equation of state (EOS). We estimate that up to $\sim 25\%$ of all BNSs may result in prompt collapse. We also find that most models of the BNS mass function we treat predict that the majority of prompt-collapse BNSs have $q \gtrsim 0.8$. Furthermore, the larger $M_{\rm thres}$ is, the more skewed toward $q = 1$ the distribution of binaries with $M_{\rm tot} > M_{\rm thres}$ becomes. Thus, most prompt-collapse BNSs may appear orphan. But, does this imply no detectable EM counterparts from such mergers?

Recent work found that interactions in compact binary magnetospheres [70–74] (see also [75–78] for related discussions) can power $\sim 10^{41-43} (B_p/10^{12}\ {\rm G})^2\ {\rm erg\ s^{-1}}$ EM signals several milliseconds prior to merger. Here B_p is the magnetic field strength at the pole of the NS. Moreover, following BH formation there is a significant amount of energy stored in the magnetosphere of the remnant. Studies of magnetospheres of stars collapsing to BHs [79–81] have shown that a fraction $\epsilon \gtrsim 1\%$ [82] of the total energy stored in a force-free magnetosphere is radiated away on a collapse timescale $\tau_{\rm FRB}$. This timescale is $\mathcal{O}(1\ {\rm ms})$ for a NS. For a magnetic dipole in flat spacetime the total magnetic energy in the magnetosphere is

$$E_{\rm B} \sim \int_R^\infty \int_0^\pi \frac{B^2}{8\pi} \left(\frac{R}{r}\right)^6 \frac{5 + 3\cos(2\theta)}{8} 2\pi r^2 \sin\theta dr d\theta \sim \frac{1}{12} B^2 R^3 \sim 10^{41} B_{12}^2 R_{10}^3\ {\rm erg}, \quad (1)$$

implying an outgoing EM luminosity of

$$L_{\rm FRB} \sim 10^{42} \epsilon_{0.01} B_{12}^2 R_{10}^3 \tau_{\rm FRB,1}^{-1}\ {\rm erg\ s^{-1}}. \quad (2)$$

Here, $B_{12} = B_p/10^{12}$ G, R_{10} the stellar radius in units of 10 km, $\epsilon_{0.01}$ the efficiency ϵ normalized to 0.01, and $\tau_{\rm FRB,1}$ the emission time in units of 1 ms. Note that for a rotating collapsing star the efficiency is $\epsilon \simeq 18\%$ [80], but here and throughout we adopt the lower value $\sim 1\%$ as a lower bound. This outgoing luminosity in Eq. (2) matches the premerger magnetospheric luminosity. Moreover, the power and duration of these magnetospheric signals match those of observed FRBs [35]. Thus, BNSs are candidates for non-repeating, FRBs, as has also been suggested in [31].

Note that when two NSs merge and promptly collapse to a BH, the total energy stored in the magnetosphere is anticipated to be of the same order of magnitude as in Eq. (2), because there is little time available to amplify the surface magnetic field through hydromagnetic instabilities as in a delayed collapse scenario [83]. However, compression due to the collision can amplify the magnetic field because of magnetic flux freezing. On the other hand, a large amount of the energy will quickly fall into the remnant BH. Thus, a detailed numerical relativity study of prompt-collapse BNS mergers is necessary to assess the postmerger magnetospheric energy of BNSs resulting in prompt collapse.

To confirm the expectation from Eq. (2), we perform fully general relativistic, ideal magnetohydrodynamics simulations of prompt-collapse BNS mergers. Following

BH formation we compute the energy stored in the magnetosphere. Assuming a 1% radiation efficiency and a millisecond emission time, we estimate an outgoing burst with luminosity $L_{\rm EM} \sim 10^{40-42}(\epsilon/0.01)(B/10^{12}\ {\rm G})^2$ erg/s, which at the edge of the LIGO BNS range translates to flux densities of 0.1 to 30 Jy—observable by existing radio telescopes. Thus, our simulations provide support to the idea that the collapse in prompt-collapse BNSs is a promising FRB counterpart to the GWs, i.e., the FRB would not be only precursor, but continue also after the peak GW amplitude.

To sum, BNS mergers are promising candidates for nonrepeating FRBs, and such FRBs *may* be the most promising EM counterpart of orphan BNS mergers. The outgoing magnetospheric burst is rather isotropic [71,72,80], in contrast to a sGRB which is beamed, making the detection of such FRB signatures largely independent of the binary orientation. Detection of an FRB can trigger searches in LIGO/Virgo data. The discovery of coincident GWs with an FRB may settle the extragalactic origin of a fraction of FRBs. Moreover, detection of an FRB from an orphan BNS merger could provide strong evidence that the merger resulted in prompt collapse to a BH, and could place constraints on the nuclear EOS, see e.g., [84,85]. Note that without an electromagnetic counterpart, a prompt-collapse BNS system might also be interpreted as a low-mass binary black hole or other dark binary compact object, because finite size effects become significant late in the binary inspiral, where current gravitational wave detectors are not as sensitive. Thus, to discern a binary black hole from a prompt-collapse BNS merger, the lack of a kilonova and sGRB is only a necessary ingredient. The FRB would be important to solidify that matter was present in the event and hence endorse information coming from GWs on finite size effects. By contrast a near equal-mass binary black hole-neutron star (BHNS) is likely to form accretion disks and eject matter more than $10^{-3}M_\odot$, and hence power detectable kilonovae. In particular, using the updated formula of [86] for the amount of mass outside the BH in a BHNS merger, we find that for an equal-mass BHNS merger, adopting a range of NS radii favored by GW170817 [87]), i.e., compactness values $C_{\rm NS} \sim 0.165$–0.205, and BH spins $\chi = 0$–0.93 more than 90% of the $C_{\rm NS} - \chi$ parameter space results in mergers with mass outside the BH exceeding $10^{-2.5}M_\odot$. Given that recent work [88–90] has shown that several tens of percent of the mass outside the BH becomes unbound due to viscous/magnetic/neutrino processes, the above imply that near equal mass BHNSs most likely power observable kilonovae, and possibly also short gamma-ray bursts. Thus, a prompt collapse BNS merger can in principle be distinguished from a BHNS merger, after the compact binary parameters have been inferred from the GW observations. In addition, a prompt collapse merger is distinguishable from a delayed collapse or no-collapse BNS merger, since numerical simulations of such mergers show that delayed collapse or no-collapse is associated with dynamical ejecta masses that are $> 0.001M_\odot$ and disk masses of a few % (see e.g., [47,66,91]). Note also, that the consensus in the community is that GW170817 was a delayed collapse merger [92–96]. Hence, BHNS, delayed collapse and no collapse BNS mergers are all anticipated to have detectable kilonovae, and thus are in all likelihood distinguishable in this respect from prompt collapse BNS mergers.

The remainder of the paper is organized as follows. In Sec. II prompt-collapse BNS mergers are motivated through a study of the BNS $M_{\rm tot}$ and q distribution. A description of our simulations and results are presented in Sec. III. Our conclusions are provided in Sec. IV. Geometrized units ($G = c = 1$) are adopted throughout, unless otherwise specified.

II. PROBABILITY ESTIMATES FOR BNS MERGERS

To assess whether prompt-collapse BNS mergers are astrophysically relevant, and in particular whether *orphan* BNS mergers are likely, we need to know the value of $M_{\rm thres}$, and the BNS $M_{\rm tot}$ and q distribution. We address these topics in this section.

A. Constraints on the threshold mass for prompt collapse

While $M_{\rm thres}$ has been found to be independent of the mass ratio [97], it is sensitive to the nuclear EOS [49,50,84,97,98], which is not very well constrained, yet. A number of studies have recently placed constraints on the nuclear EOS using the observation of GW170817 (see, e.g., [99] and references therein as well as [100,101] for reviews). Here we focus on works that set constraints on the Tolman-Oppenheimer-Volkoff (TOV) limit ($M_{\rm TOV}$), i.e., the maximum mass supported by a nonrotating NS. In particular, [92–95] following different approaches concluded that GW170817 sets an upper bound $M_{\rm TOV} \lesssim 2.2M_\odot$ ([94] argues for $M_{\rm TOV} \lesssim 2.17M_\odot$ at 90% confidence). We now use the upper bound on $M_{\rm TOV}$ to obtain a reasonable range for $M_{\rm thres}$.

In [84] $M_{\rm thres}$ was computed for a number of realistic, finite temperature EOSs, and was found that $M_{\rm thres} \in [2.95, 3.85]\ M_\odot$. However, if we demand that the EOS respect $M_{\rm TOV} \lesssim 2.2M_\odot$, then the range shrinks to $M_{\rm thres} \in [2.95, 3.25]\ M_\odot$ for the EOSs considered in [84].

In addition, [84] derived the following EOS-independent relation that expresses $M_{\rm thres}$ in terms of $M_{\rm TOV}$ [102]

$$M_{\rm thres} = (aC^*_{1.6} + b)M_{\rm TOV}, \tag{3}$$

where $a = -3.606$, $b = 2.380$, and $C^*_{1.6} = M_{\rm TOV}/R^*_{1.6}$, with $R^*_{1.6}$ the radius of a $1.6M_\odot$ NS for a given EOS. We note that $M_{\rm thres}$ here is defined as the Arnowitt-Deser-Misner (ADM) mass of the binary, if the binary companions were

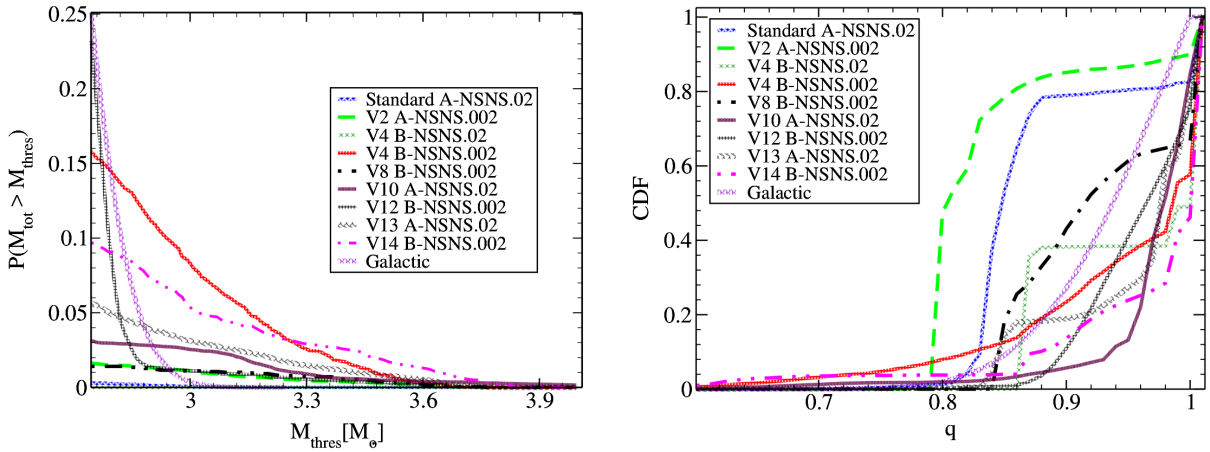

FIG. 1. Left: Probability for $M_{\rm tot} > M_{\rm thres}$, where $M_{\rm tot}$ is the binary ADM mass, if the binary components were infinitely separated. The curves labeled "##-#NSNS.###" correspond to population synthesis calculations, and the curve labeled "Galactic" corresponds to the mass distribution of Eq. (4). Right: the cumulative distribution function (CDF) for the mass ratio that corresponds to the same models shown on the left.

infinitely separated. We can use Eq. (3) in conjunction with the EOSs that are favored by GW170817 [87] to explore how small the lower bound on $M_{\rm thres}$ can become. We investigated the masses and radii of cold nuclear EOSs listed in [103]. Among the EOSs that respect $1.97M_\odot \lesssim M_{\rm TOV} \lesssim 2.2M_\odot$ [104], and the mass-radius constraints of [87], the EOS WFF1 [105] yields a smallest value for $M_{\rm thres}$ through Eq. (3); namely, $M_{\rm thres} \simeq 2.75M_\odot$. This is not unexpected because Eq. (3) predicts that the softer the EOS (larger $C^*_{1.6}$) and the smaller $M_{\rm TOV}$ are, the smaller $M_{\rm tresh}$ becomes. WFF1 is among the softest EOSs with $M_{\rm TOV} \sim 2.0M_\odot$. Thus, in this work we adopt $[2.75, 3.25]\ M_\odot$ as a reasonable range for $M_{\rm thres}$ respecting current constraints on the nuclear EOS.

B. Binary neutron star total mass and mass-ratio distributions

The NS mass function for Galactic BNSs has been modeled in [106,107]. As in [108], in our analysis below we use the Gaussian mass function of [107], because it is simpler to work with and because the skewed Gaussian of [106] is consistent with 0 skewness parameter, and hence agrees very well with the distribution of [107]. In [107] the probability distribution function of NS masses ($M_{\rm NS}$) in Galactic BNSs is modeled as

$$P(M_{\rm NS}; M_0, \sigma) = \frac{1}{2\pi\sigma^2} \exp\left[-\frac{(M_{\rm NS} - M_0)^2}{2\sigma^2}\right] \quad (4)$$

with $M_0 = 1.33M_\odot$, and $\sigma = 0.09M_\odot$. Assuming that the masses of the two NSs in a BNS are independent random variables, we can use Eq. (4) to derive the distribution of the BNS $M_{\rm tot}$ and that of q. The $M_{\rm tot}$ distribution is again given by Eq. (4), but with $M_0 = 2.66M_\odot$, $\sigma = 0.09 \times \sqrt{2}\ M_\odot$, and $M_{\rm NS}$ replaced with $M_{\rm tot}$. Using the $M_{\rm tot}$ distribution we can compute the probability that $M_{\rm tot}$ is greater than a certain value. In the left panel of Fig. 1 this is shown by the curve labeled "Galactic," which demonstrates that if $M_{\rm thres} = 2.75M_\odot$, as in the WFF1 EOS, then ~25% of all binaries result in prompt collapse. However, if $M_{\rm thres} = 3.25M_\odot$ (the upper value in the range we discussed in the previous subsection), then the Galactic NS mass function predicts that there are practically no BNSs resulting in prompt collapse. If we use $M_{\rm thres} \simeq 2.8$ [52], which corresponds to the SLy [109] and APR4 [110] EOSs, also favored by GW170817 [87], then the Galactic NS mass function predicts that ~13.5% of all BNSs result in prompt collapse.

The Galactic mass function may not be representative of all BNSs. Thus, we also use results from population synthesis studies [111]. In the left panel of Fig. 1 we show the probability that $M_{\rm tot} > M_{\rm thres}$ for one of the standard models of [111] labeled "Standard," and several variations of the standard models labeled "##-#NSNS.###" (see [111,112] for the labeling and what parameters are varied). The conclusion from the plot is that there are realizations with a wide tail at large $M_{\rm tot}$, for which a significant fraction of BNSs result in prompt collapse (even for $M_{\rm thres} = 3.25M_\odot$). However, there exist realizations for which there are practically no BNSs with $M_{\rm tot} > M_{\rm thres}$ (even for $M_{\rm thres} = 2.75M_\odot$). But, the fact that GW170817 favors softer EOSs, makes prompt-collapse BNS mergers potentially observationally relevant.

Next we address whether any orphan prompt-collapse mergers are expected. As mentioned above, we anticipate that prompt-collapse BNS mergers will eject appreciable matter and form disks for $q < 0.8$. Using Eq. (4) for the Galactic NS mass distribution in BNSs we can compute the q distribution of BNSs. In the right panel of Fig. 1 we show the cumulative distribution of q for Milky-way like BNSs labeled "Galactic." Thus, for the Galactic mass function more than ~80% of BNSs have $q > 0.9$. We have also

checked that this result holds even when restricting to binaries with $M_{\rm tot}$ greater than $M_{\rm thres} \in [2.75M_\odot, 3.25M_\odot]$. Moreover, we find that for larger $M_{\rm thres}$, the q distribution of $M_{\rm tot} > M_{\rm thres}$ binaries is skewed even more toward $q = 1$. This result is explained as follows: the number of very high mass NSs is very low, and achieving $M_{\rm tot}$ more than $\sim 3.00M_\odot$ requires $q \sim 1$ binaries.

The q distribution from select population synthesis models is also shown in the right panel of Fig. 1. It is clear that $q \gtrsim 0.8$ in most cases, and there exist realizations where more than ~90% of BNSs have $q > 0.95$. We have also checked that these results hold, even when restricting to binaries with $M_{\rm tot} > M_{\rm thres}$. As in the Galactic case, we find in the population synthesis results, too, that the larger $M_{\rm thres}$ is, the more symmetric binaries with $M_{\rm tot} > M_{\rm thres}$ become. In particular of all 60 variations of populations synthesis models available in [112], we find that for $M_{\rm tot} > M_{\rm thres}$ only 17, 15 and 3 variations have 20% or more binaries with $q < 0.8$, for $M_{\rm thres} = 2.75$, 2.95, and $3.25M_\odot$, respectively.

These results and the discussion in the previous section suggest that the majority of prompt-collapse BNS mergers are likely to appear orphan, and hence their most promising EM counterpart likely will arise by magnetospheric effects, and may be a nonrepeating FRB.

III. SIMULATIONS AND RESULTS

We performed fully general relativistic, ideal magnetohydrodynamic simulations of BNSs endowed with an initial dipole magnetosphere to assess whether prompt-collapse BNSs have enough energy stored in the remnant magnetosphere to power an FRB. We adopt the code of [113–115]. Our evolution methods and grid set up are the same as those described in [53]. The initial data we adopt are publicly available, have been generated with the LORENE library [116] and correspond to cases P-Prompt-1, P-Prompt-2, and P-Prompt-3 of [53]. These are $\Gamma = 2$ polytropic [117], irrotational BNS initial data. We seed an initial dipole magnetic field in each NS by use of Eq. (2) of [72]. The resulting magnetic field configuration is the same as in [53], but we set the initial polar magnetic field (as measured by comoving observers) to $B_p = 10^{12}$ G. This initial magnetic field is dynamically unimportant, thus our simulations scale with B_p. In our results below we show the scaling with $B_{12} = B_p/10^{12}$ G. To mimic the force-free conditions in NS magnetospheres we adopt the method we developed in [18] where at $t = 0$ we impose a low but variable density atmosphere with a universal plasma parameter beta less than unity. The value of the plasma beta is 0.01, and this captures one key aspect of force-free electrodynamics, i.e., magnetic field pressure dominance. As explained in [18] our code can handle such values of plasma parameter beta [118].

The basic dynamics of these systems has been described in [53] where it was shown that these systems form negligibly small disks onto the remnant BH and no jets are launched. We terminate our simulations when the electromagnetic energy outside the remnant BH has settled. We compute the energy stored in the magnetosphere as measured by comoving observers as in Eq. (9) of [53]. At any given time we compute the magnetospheric energy (E_B) only below a certain rest-mass density which we set to 10^{-4} of the maximum rest-mass density on the grid at that time. For case P-Prompt-3 we also changed this value to 10^{-5} of the maximum density to test if this choice makes a difference. We call this case P-Prompt-3*. We list the measured energy in the magnetosphere outside the BH after it has settled in Table I. As is clear from the table the energy matches well the order-of-magnitude predictions of Eq. (1).

TABLE I. Summary of main results. Here E_B is the magnetic energy stored in the magnetosphere as measured by observers comoving with the plasma $t \sim 200M$ following BH formation. $L_{\rm FRB}$ is the estimated luminosity produced by the ejection of 0.8% of the magnetic energy stored in the magnetosphere in $\tau_{\rm FRB} = 1$ ms. S_ν is the flux density at the detector in units of Jy assuming a nominal observing frequency of 1 GHz and that the source is located at the edge of the LIGO BNS range, i.e., 200 Mpc. Units are assigned by setting the polytropic constant $k = 262.7$ km^2.

Case model	E_B/B_{12}^2 [erg]	$L_{\rm FRB}/(B_{12}^2\tau_{\rm FRB,1}^{-1})$ [erg s^{-1}]	S_ν [Jy] at $\nu = 1$ GHz
P-Prompt-1	$10^{40.9}$	$10^{41.8}$	13.2
P-Prompt-2	$10^{38.9}$	$10^{39.8}$	0.13
P-Prompt-3	$10^{41.3}$	$10^{42.2}$	33.1

In Fig. 2 we show the time evolution of the EM energy in the magnetosphere for each case we considered. The plot exhibits that after an initial settling of the magnetosphere, the magnetospheric energy is approximately constant until merger, at which point it increases by about a factor of 2 by the collision, and subsequently decays, as part of the magnetosphere flows into the remnant BH. Cases P-Prompt-3 and P-Prompt-3* demonstrate that changing the cut-off density by an order of magnitude for the computation of the electromagnetic energy in the magnetosphere has an effect that is less than 5% up to $200M$ following BH formation when the EM has already approximately settled.

It is not clear where the difference in the electromagnetic energy in the magnetospheres in the 3 cases we study is coming from. However, the different configurations undergo collapse in different ways, because P-prompt-2 is much more massive than the other two cases, and P-prompt-1 is asymmetric. It is likely that the more "violent" collapse of case P-prompt-2 drags a larger part of the magnetosphere through the horizon leaving less electromagnetic energy exterior to the BH. This suggests that the "promptness" of the collapse may determine the amount of energy in the magnetosphere. More detailed

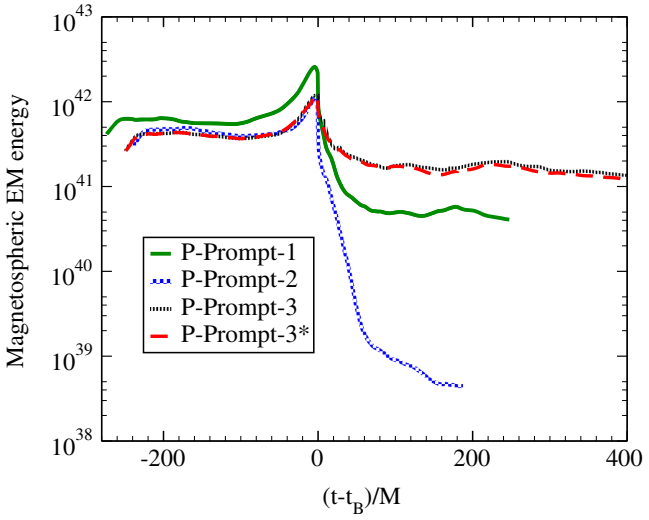

FIG. 2. Time evolution of electromagnetic energy in the magnetosphere for the 4 cases studied in this work. The time axis is shifted with respect to the time of BH formation t_B and is normalized to the ADM mass of the system. Physical units are assigned by setting the polytropic constant $k = 262.7$ km^2.

studies are necessary to solidify this explanation, and these will be the subject of future work.

To estimate the outgoing EM luminosity that is expected to be produced by the "release" of the magnetosphere, we assume that a fraction $\epsilon = 0.8\%$ of E_B is radiated away in $\tau_{\rm FRB} = 1$ ms. The efficiency ϵ we adopt is motivated by [80]. The outgoing EM luminosity is estimated as

$$L_{\rm FRB} \sim \epsilon \frac{E_B}{\tau_{\rm FRB}} \simeq 10^{42} \epsilon_{0.008} B_{12}^2 \tau_{\rm FRB,1}^{-1} \ {\rm erg\,s^{-1}}. \quad (5)$$

The $L_{\rm FRB}$ estimate for each case we simulate is listed in Table I. We also convert the luminosity to observed flux density (S_ν) at the detector in units of Jy using $S_\nu = L_{\rm FRB}/4\pi D^2/\nu$, where D is the luminosity distance to the source, ν the radio telescope observing frequency. The flux density equation can be written as

$$S_\nu \simeq 2.1\,{\rm Jy} \left(\frac{L_{\rm FRB}}{10^{41}\,{\rm erg\,s^{-1}}}\right) \left(\frac{D}{200\,{\rm Mpc}}\right)^{-2} \left(\frac{\nu}{1\,{\rm GHz}}\right)^{-1}, \quad (6)$$

where we chose a nominal observing frequency of 1 GHz (as is typical of observed FRBs), and placed the source at the edge of the LIGO BNS range. As shown in Table I the expected burst of the EM radiation for a source at 200 Mpc has flux densities ∼0.1–30 Jy and is fully consistent with observed FRB flux densities [35] that have been detected by current radio telescopes such as CHIME, UTMOST, ASKAP, Parkes, and Arecibo.

We stress that the FRB in the model discussed here is not coming from the collapse only. The inspiral magnetospheric interactions contribute, making it possible to match the observed durations of FRBs, the longest of which are challenging to match by the collapse alone. The luminosity of the emission prior to merger [70–74] is comparable to the postcollapse burst. We note while we were writing our paper, the idea of an FRB from the prompt collapse alone was also suggested in [119].

IV. CONCLUSIONS

In this paper, we performed a statistical study of the total mass and mass ratio distribution of BNSs using the Galactic NS mass function and population synthesis models in conjunction with recent constraints on the nuclear EOS from GW170817. We find that up to ∼25% of all BNS mergers could result in prompt collapse. Moreover, our analysis shows that most of the considered models of the BNS mass function predict that the majority of prompt-collapse BNS mergers have $q \gtrsim 0.8$, and that the larger $M_{\rm thres}$ is, the closer to unity the q distribution of prompt-collapse binaries approaches. Prompt-collapse BNSs with $q > 0.8$ are likely to unbind a negligible amount of mass, and form negligibly small disks onto the remnant BHs. Thus, neither detectable kilonovae nor sGRBs may accompany the GWs from such prompt collapse BNSs. We referred to these kilonovae- and sGRB-free BNS mergers as orphan. Our statistical study suggests that most prompt-collapse BNS mergers may be orphan. Therefore, the only remaining viable mechanism for powering detectable electromagnetic counterparts from orphan BNS mergers is related to magnetospheric effects.

We argued that the release of energy stored in the magnetosphere of the merger remnant can match the *duration and power* of some FRBs and that it also matches the luminosity of premerger magnetospheric interactions. Thus, BNS mergers are promising sources of detectable, nonrepeating FRBs, as has been suggested before, and FRBs *may* be the most promising electromagnetic counterpart of orphan BNS mergers. The outgoing magnetospheric burst in these cases is rather isotropic, making the detection of coincident FRB and GW signatures possible. However, the most likely channel for such coincident detections would be searches in LIGO data triggered by FRB detections, because it is impossible for radio telescopes to follow up GW detections on ms timescales.

We have also performed magnetohydrodynamic simulations in full general relativity of different BNS configurations that undergo *prompt* collapse. The stars are initially seeded with a dipolar magnetic field that extends from the NS interior into the exterior. We computed the energy stored in the magnetosphere following BH formation, and estimated the outgoing electromagnetic luminosity produced. We find luminosities $L_{\rm FRB} \sim 10^{40-42} B_{12}^2$ erg s^{-1}, which at the edge of the LIGO BNS range translate to flux densities of 0.1 to 30 Jy, matching the flux density of previously observed FRBs.

We close with a few caveats: First, our statistical analysis can be refined as soon as ground based GW interferometers unveil the NS mass function in BNSs; second if one is interested in the LIGO/Virgo *observed* mass function, the delay-time distribution should be considered, which we do not account for here; third, some conclusions in our work are based on the size of ejecta and BH disks found in numerical relativity simulations of prompt-collapse BNS mergers. The number of such simulations is small compared to simulations of BNS mergers resulting in delayed collapse. Therefore, more high-resolution simulations in full general relativity of BNSs resulting in prompt collapse are necessary to solidify the results that such mergers unbind negligible amounts of mass and form negligibly small disks onto the remnant BH, and to find the "critical" mass ratio below which appreciable mass ejection and disks occur. This critical mass ratio is also likely to be equation-of-state dependent. Fourth, whether an FRB signature from magnetospheric effects is luminous enough depends on the NS surface magnetic field. We adopted a value of $\sim 10^{12}$ G, but FRB-level luminosities from magnetospheric interactions are possible even from $\sim 10^{11}$ G [70]. Whether such regular pulsar magnetic fields are present in these cases it is unclear, and this introduces a source of uncertainty. If BNSs were to have only low magnetic fields, this could make prompt-collapse BNS mergers completely orphan from an electromagnetic point of view. However, on evolutionary grounds one of the two components in a field BNS (i.e., not one that forms dynamically in a cluster) is always anticipated to have a magnetic field of $\sim 10^{11-12}$ G. This is because the NS that forms second is not recycled, and hence its magnetic field is not "buried" during a recycling process, see, e.g., [120] for a review. In fact, the double pulsar J0737-3039 has provided a spectacular confirmation of the evolutionary theory of double NSs [120]. Pulsar B in J0737-3039 has an inferred magnetic field of 1.6×10^{12} G [121], while pulsar A is a millisecond pulsar and has an inferred magnetic field of 6×10^{9} G. In addition, the pulsar in the double NS J1906 + 0746 has an inferred magnetic field strength 1.8×10^{12} G [122]. Note that for stronger, near magnetar-level magnetic fields a precursor burst of gamma-rays is possible from BNS mergers [123]. Another source of uncertainty is that to explain FRBs we need to know the efficiency for converting the total magnetospheric power output to radio waves. If this efficiency is less than 1%, then it is not likely that FRBs can be accounted for by magnetospheric effects. Finally, with our code we are able to obtain only crude estimates of the energy in the magnetosphere. A more accurate assessment of the full FRB signature in the model considered here requires a code (such as that of [70,71]) that can evolve through inspiral, merger and prompt collapse to magnetosphere release, while smoothly matching the ideal magnetohydrodynamic stellar interior to a force-free exterior. Such a simulation is currently lacking and will be the subject of future work of ours.

ACKNOWLEDGMENTS

We thank Richard O'Shaughnessy for pointing us to the Synthetic Universe website. We also thank S. L. Shapiro and R. Thompson for useful discussions. This work has been supported in part by National Science Foundation (NSF) Grant No. PHY-1912619 at the University of Arizona, NSF Grants No. PHY-1602536 and No. PHY-1662211, and NASA Grant No. 80NSSC17K0070 at the University of Illinois at Urbana-Champaign. Simulations were in part run on the Perseus cluster at Princeton University. This work made use of the Extreme Science and Engineering Discovery Environment (XSEDE) under Grants No. TG-PHY180036 and No. TG-PHY190020.

[1] B. P. Abbott *et al.* (LIGO Scientific and Virgo Collaborations), Phys. Rev. Lett. **116**, 061102 (2016).
[2] B. P. Abbott *et al.* (Virgo and LIGO Scientific Collaborations), Phys. Rev. Lett. **116**, 241103 (2016).
[3] B. P. Abbott *et al.* (Virgo and LIGO Scientific Collaborations), Phys. Rev. Lett. **118**, 221101 (2017).
[4] B. P. Abbott *et al.* (Virgo and LIGO Scientific Collaborations), Phys. Rev. Lett. **119**, 141101 (2017).
[5] B. P. Abbott *et al.* (Virgo and LIGO Scientific Collaborations), Astrophys. J. **851**, L35 (2017).
[6] B. P. Abbott *et al.* (LIGO Scientific and Virgo Collaborations), arXiv:1811.12940.
[7] B. P. Abbott *et al.* (Virgo and LIGO Scientific Collaborations), Phys. Rev. Lett. **119**, 161101 (2017).
[8] B. P. Abbott *et al.* (Virgo, Fermi-GBM, INTEGRAL, and LIGO Scientific Collaborations), Astrophys. J. **848**, L13 (2017).
[9] B. P. Abbott *et al.*, Astrophys. J. **848**, L12 (2017).
[10] D. Eichler, M. Livio, T. Piran, and D. N. Schramm, Nature (London) **340**, 126 (1989).
[11] R. Narayan, B. Paczynski, and T. Piran, Astrophys. J. Lett. **395**, L83 (1992).
[12] B. Paczynski, Astrophys. J. Lett. **308**, L43 (1986).
[13] T. Piran, in *Proceedings of the 16th International Conference, Durban, South Africa, 2001*, edited by N. T. Bishop and D. M. Sunil (World Scientific, Singapore, 2002), p. 259.
[14] E. Berger *et al.*, Nature (London) **438**, 988 (2005).

[15] D. Fox *et al.*, Nature (London) **437**, 845 (2005).
[16] J. Hjorth *et al.*, Nature (London) **437**, 859 (2005).
[17] J. S. Bloom *et al.*, Astrophys. J. **638**, 354 (2006).
[18] V. Paschalidis, M. Ruiz, and S. L. Shapiro, Astrophys. J. Lett. **806**, L14 (2015).
[19] M. Ruiz, R. N. Lang, V. Paschalidis, and S. L. Shapiro, Astrophys. J. **824**, L6 (2016).
[20] L. Baiotti and L. Rezzolla, Rep. Prog. Phys. **80**, 096901 (2017).
[21] V. Paschalidis, Classical Quantum Gravity **34**, 084002 (2017).
[22] J. M. Lattimer and D. N. Schramm, Astrophys. J. Lett. **192**, L145 (1974).
[23] L.-X. Li and B. Paczynski, Astrophys. J. **507**, L59 (1998).
[24] D. R. Lorimer, M. Bailes, M. A. McLaughlin, D. J. Narkevic, and F. Crawford, Science **318**, 777 (2007).
[25] D. Thornton *et al.*, Science **341**, 53 (2013).
[26] See http://www.astronomy.swin.edu.au/pulsar/frbcat for an up-to-date-catalog of FRBs.
[27] L. G. Spitler *et al.*, Nature (London) **531**, 202 (2016).
[28] A. Josephy *et al.*, arXiv:1906.11305 [Astrophys. J. Lett. (to be published)].
[29] M. Amiri *et al.* (CHIME/FRB Collaboration), Nature (London) **566**, 235 (2019).
[30] S. B. Popov and K. A. Postnov, arXiv:0710.2006 [Mon. Not. Roy. Astron. Soc. (to be published)].
[31] T. Totani, Publ. Astron. Soc. Jpn. **65**, L12 (2013).
[32] H. Falcke and L. Rezzolla, Astron. Astrophys. **562**, A137 (2014).
[33] J. Bramante and T. Linden, Phys. Rev. Lett. **113**, 191301 (2014).
[34] I. I. Tkachev, JETP Lett. **101**, 1 (2015).
[35] C. M. F. Mingarelli, J. Levin, and T. J. W. Lazio, Astrophys. J. **814**, L20 (2015).
[36] S. L. Liebling and C. Palenzuela, Phys. Rev. D **94**, 064046 (2016).
[37] B. Marcote *et al.*, Astrophys. J. **834**, L8 (2017).
[38] F. Zhang, Astron. Astrophys. **598**, A88 (2017).
[39] M. Nicholl, P. K. G. Williams, E. Berger, V. A. Villar, K. D. Alexander, T. Eftekhari, and B. D. Metzger, Astrophys. J. **843**, 84 (2017).
[40] J. P. Conlon and C. A. R. Herdeiro, Phys. Lett. B **780**, 169 (2018).
[41] S. Yamasaki, T. Totani, and K. Kiuchi, Publ. Astron. Soc. Jpn. **70**, 39 (2018).
[42] A. L. Piro, B. Giacomazzo, and R. Perna, Astrophys. J. **844**, L19 (2017).
[43] B. Margalit, B. D. Metzger, E. Berger, M. Nicholl, T. Eftekhari, and R. Margutti, Mon. Not. R. Astron. Soc. **481**, 2407 (2018).
[44] E. R. Most, A. Nathanail, and L. Rezzolla, Astrophys. J. **864**, 117 (2018).
[45] B. D. Metzger, Living Rev. Relativity **20**, 3 (2017).
[46] G. Ghirlanda *et al.*, Pub. Astron. Soc. Aust. **31**, e022 (2014).
[47] K. Hotokezaka, K. Kiuchi, K. Kyutoku, H. Okawa, Y.-i. Sekiguchi, M. Shibata, and K. Taniguchi, Phys. Rev. D **87**, 024001 (2013).
[48] T. Dietrich, M. Ujevic, W. Tichy, S. Bernuzzi, and B. Bruegmann, Phys. Rev. D **95**, 024029 (2017).
[49] M. Shibata, K. Taniguchi, and K. Uryū, Phys. Rev. D **68**, 084020 (2003).
[50] M. Shibata, K. Taniguchi, and K. Uryū, Phys. Rev. D **71**, 084021 (2005).
[51] Y. T. Liu, S. L. Shapiro, Z. B. Etienne, and K. Taniguchi, Phys. Rev. D **78**, 024012 (2008).
[52] K. Hotokezaka, K. Kyutoku, H. Okawa, M. Shibata, and K. Kiuchi, Phys. Rev. D **83**, 124008 (2011).
[53] M. Ruiz and S. L. Shapiro, Phys. Rev. D **96**, 084063 (2017).
[54] M. Ruiz, A. Tsokaros, V. Paschalidis, and S. L. Shapiro, Phys. Rev. D **99**, 084032 (2019).
[55] D. A. Coulter *et al.*, Science **358**, 1556 (2017).
[56] M. R. Drout *et al.*, Science **358**, 1570 (2017).
[57] B. J. Shappee *et al.*, Science **358**, 1574 (2017).
[58] M. M. Kasliwal *et al.*, Science **358**, 1559 (2017).
[59] M. Tanaka *et al.*, Publ. Astron. Soc. Jpn. **69**, 102 (2017).
[60] I. Arcavi *et al.*, Nature (London) **551**, 64 (2017).
[61] E. Pian *et al.*, Nature (London) **551**, 67 (2017).
[62] S. J. Smartt *et al.*, Nature (London) **551**, 75 (2017).
[63] M. Soares-Santos *et al.* (Dark Energy Camera GW-EM and DES Collaboration), Astrophys. J. **848**, L16 (2017).
[64] M. Nicholl *et al.*, Astrophys. J. **848**, L18 (2017).
[65] P. S. Cowperthwaite *et al.*, Astrophys. J. **848**, L17 (2017).
[66] D. Radice, A. Perego, F. Zappa, and S. Bernuzzi, Astrophys. J. **852**, L29 (2018).
[67] Such small ejecta masses constitute ∼0.01% of the total rest-mass and it is not clear that numerical relativity simulations have achieved such high levels of accuracy, yet.
[68] B. D. Metzger and E. Berger, Astrophys. J. **746**, 48 (2012).
[69] L. Rezzolla, L. Baiotti, B. Giacomazzo, D. Link, and J. A. Font, Classical Quantum Gravity **27**, 114105 (2010).
[70] C. Palenzuela, L. Lehner, M. Ponce, S. L. Liebling, M. Anderson, D. Neilsen, and P. Motl, Phys. Rev. Lett. **111**, 061105 (2013).
[71] C. Palenzuela, L. Lehner, S. L. Liebling, M. Ponce, M. Anderson, D. Neilsen, and P. Motl, Phys. Rev. D **88**, 043011 (2013).
[72] V. Paschalidis, Z. B. Etienne, and S. L. Shapiro, Phys. Rev. D **88**, 021504 (2013).
[73] M. Ponce, C. Palenzuela, L. Lehner, and S. L. Liebling, Phys. Rev. D **90**, 044007 (2014).
[74] M. Ponce, C. Palenzuela, E. Barausse, and L. Lehner, Phys. Rev. D **91**, 084038 (2015).
[75] B. M. Hansen and M. Lyutikov, Mon. Not. R. Astron. Soc. **322**, 695 (2001).
[76] S. T. McWilliams and J. Levin, Astrophys. J. **742**, 90 (2011).
[77] A. L. Piro, Astrophys. J. **755**, 80 (2012).
[78] D. Lai, Astrophys. J. **757**, L3 (2012).
[79] T. W. Baumgarte and S. L. Shapiro, Astrophys. J. **585**, 930 (2003).
[80] L. Lehner, C. Palenzuela, S. L. Liebling, C. Thompson, and C. Hanna, Phys. Rev. D **86**, 104035 (2012).
[81] K. Dionysopoulou, D. Alic, C. Palenzuela, L. Rezzolla, and B. Giacomazzo, Phys. Rev. D **88**, 044020 (2013).
[82] The fraction is 20% for electrovacuum [79].

[83] K. Kiuchi, P. Cerd-Durn, K. Kyutoku, Y. Sekiguchi, and M. Shibata, Phys. Rev. D **92**, 124034 (2015).
[84] A. Bauswein, T. W. Baumgarte, and H. T. Janka, Phys. Rev. Lett. **111**, 131101 (2013).
[85] Note that if one knows the collapse time from merger constraints on the EOS can be placed using sGRBs [124], too.
[86] F. Foucart, T. Hinderer, and S. Nissanke, Phys. Rev. D **98**, 081501 (2018).
[87] B. P. Abbott *et al.* (LIGO Scientific and Virgo Collaboration), Phys. Rev. Lett. **121**, 161101 (2018).
[88] D. Kasen, R. Fernandez, and B. Metzger, Mon. Not. R. Astron. Soc. **450**, 1777 (2015).
[89] R. Fernndez and B. D. Metzger, Annu. Rev. Nucl. Part. Sci. **66**, 23 (2016).
[90] D. M. Siegel and B. D. Metzger, Phys. Rev. Lett. **119**, 231102 (2017).
[91] W. E. East, V. Paschalidis, F. Pretorius, and A. Tsokaros, arXiv:1906.05288 [Phys. Rev. D (to be published)].
[92] M. Ruiz, S. L. Shapiro, and A. Tsokaros, Phys. Rev. D **97**, 021501 (2018).
[93] L. Rezzolla, E. R. Most, and L. R. Weih, Astrophys. J. **852**, L25 (2018).
[94] B. Margalit and B. D. Metzger, Astrophys. J. Lett. **850**, L19 (2017).
[95] M. Shibata, S. Fujibayashi, K. Hotokezaka, K. Kiuchi, K. Kyutoku, Y. Sekiguchi, and M. Tanaka, Phys. Rev. D **96**, 123012 (2017).
[96] A. Bauswein, O. Just, H.-T. Janka, and N. Stergioulas, Astrophys. J. **850**, L34 (2017).
[97] M. Shibata and K. Taniguchi, Phys. Rev. D **73**, 064027 (2006).
[98] A. Bauswein and N. Stergioulas, Mon. Not. R. Astron. Soc. **471**, 4956 (2017).
[99] V. Paschalidis, K. Yagi, D. Alvarez-Castillo, D. B. Blaschke, and A. Sedrakian, Phys. Rev. D **97**, 084038 (2018).
[100] C. A. Raithel, Eur. Phys. J. A **55**, 80 (2019).
[101] S. Gandolfi, J. Lippuner, A. W. Steiner, I. Tews, X. Du, and M. Al-Mamun, arXiv:1903.06730.
[102] An expression $M_{\rm thres} = kM_{\rm TOV}$ was first proposed by [49].
[103] J. S. Read, B. D. Lackey, B. J. Owen, and J. L. Friedman, Phys. Rev. D **79**, 124032 (2009).
[104] The lower limit comes from the $2M_\odot$ pulsar observations [125,126].
[105] R. B. Wiringa, V. Fiks, and A. Fabrocini, Phys. Rev. C **38**, 1010 (1988).
[106] B. Kiziltan, A. Kottas, M. D. Yoreo, and S. E. Thorsett, Astrophys. J. **778**, 66 (2013).
[107] F. zel and P. Freire, Annu. Rev. Astron. Astrophys. **54**, 401 (2016).
[108] H. Yang, V. Paschalidis, K. Yagi, L. Lehner, F. Pretorias, and N. Yunes, Phys. Rev. D **97**, 024049 (2018).
[109] F. Douchin and P. Haensel, Astron. Astrophys. **380**, 151 (2001).
[110] A. Akmal, V. R. Pandharipande, and D. G. Ravenhall, Phys. Rev. C **58**, 1804 (1998).
[111] M. Dominik, K. Belczynski, C. Fryer, D. Holz, E. Berti, T. Bulik, I. Mandel, and R. O'Shaughnessy, Astrophys. J. **759**, 52 (2012).
[112] https://www.syntheticuniverse.org/.
[113] Z. B. Etienne, V. Paschalidis, Y. T. Liu, and S. L. Shapiro, Phys. Rev. D **85**, 024013 (2012).
[114] Z. B. Etienne, Y. T. Liu, V. Paschalidis, and S. L. Shapiro, Phys. Rev. D **85**, 064029 (2012).
[115] B. D. Farris, R. Gold, V. Paschalidis, Z. B. Etienne, and S. L. Shapiro, Phys. Rev. Lett. **109**, 221102 (2012).
[116] http://www.lorene.obspm.fr.
[117] The EOS is $P = k\rho_0^\Gamma$ with P the pressure, ρ_0 the rest-mass density, and k, Γ the polytropic constant and exponent, respectively.
[118] Note that as shown in [127,128] force-free electrodynamics is a subset of ideal magnetohydrodynamics. Thus in principle a perfect ideal magnetohydrodynamics (MHD) code can also model force-free environments. However, limitations in current numerical schemes of ideal MHD do not allow the evolution of highly magnetized matter. But, they do allow the evolution of moderately magnetized matter.
[119] A. Nathanail, Galaxies **6**, 119 (2018).
[120] D. R. Lorimer, Living Rev. Relativity **11**, 8 (2008).
[121] A. G. Lyne, M. Burgay, M. Kramer, A. Possenti, R. N. Manchester, F. Camilo, M. A. McLaughlin, D. R. Lorimer, N. D'Amico, B. C. Joshi, J. Reynolds, and P. C. C. Freire, Science **303**, 1153 (2004).
[122] J. van Leeuwen *et al.*, Astrophys. J. **798**, 118 (2015).
[123] B. D. Metzger and C. Zivancev, Mon. Not. R. Astron. Soc. **461**, 4435 (2016).
[124] P. D. Lasky, B. Haskell, V. Ravi, E. J. Howell, and D. M. Coward, Phys. Rev. D **89**, 047302 (2014).
[125] P. B. Demorest, T. Pennucci, S. M. Ransom, M. S. E. Roberts, and J. W. T. Hessels, Nature (London) **467**, 1081 (2010).
[126] J. Antoniadis *et al.*, Science **340**, 1233232 (2013).
[127] J. C. McKinney, Mon. Not. R. Astron. Soc. **367**, 1797 (2006).
[128] V. Paschalidis and S. L. Shapiro, Phys. Rev. D **88**, 104031 (2013).